S-matrix, resonances, and wave functions for transport through billiards with leads

S. Albeverio
Institut für Mathematik, Ruhr-Universität Bochum, Germany, SFB 237 Essen-Bochum-Düsseldorf, Germany, BiBoS Research Center, D 33615 Bielefeld, Germany, and CERFIM, Locarno, Switzerland

F. Haake
Fachbereich Physik, Universität-GH Essen, 45117 Essen, Germany and SFB 237 Essen-Bochum-Düsseldorf, Germany

P. Kurasov
Institut für Mathematik, Ruhr-Universität Bochum, Germany, Department of Mathematical and Computational Physics, St. Petersburg University, 198904 St. Petersburg, Russia, Department of Mathematics, Stockholm University, 10691 Stockholm, Sweden, and Department of Mathematics, Luleå University, 97187 Luleå, Sweden

M. Kuś
Fachbereich Physik, Universität-GH Essen, 45117 Essen, Germany, SFB 237 Essen-Bochum-Düsseldorf, Germany, and Center for Theoretical Physics, Polish Academy of Sciences, 02-668 Warszawa, Poland

P. Šeba
Nuclear Physics Institute, Czech Academy of Sciences, 250 68 Řež near Prague, Czech Republic

(Received 17 May 1996; accepted for publication 17 June 1996)

For a simple model describing the *S*-matrices of open resonators the statistical properties of the resonances are investigated, as well as the wave functions inside the resonator. © *1996 American Institute of Physics.* [S0022-2488(96)00610-X]

I. INTRODUCTION

The properties of ballistic electron transport through a mesoscopic quantum dot are of considerable interest both experimentally and theoretically.[1,2] For the character of the electron motion the shape of the quantum dot is of particular importance. The transport characteristics—such as the conductance fluctuations—are different for shapes which correspond to integrable and chaotic classical motion inside the dot.[3] Similar results have been obtained also in experiments with microwave resonators.[4,5]

The theory accounting for this phenomena is usually based on the so-called stochastic approach, which is able to reproduce the scattering characteristics of the system[6] employing the theory of random matrices. Our aim here is to develop a simple model which will be able to describe not only the corresponding *S*-matrix but also give information about the structure of the wave function inside the cavity.

The system we would like to investigate consists of a cavity (quantum dot, electromagnetic resonator) with attached leads (antenna). The cavity is assumed to be either integrable or fully chaotic. In particular the following characteristics of the system will be of interest for us:

(1) The structure of the *S*-matrix.

(2) Statistical properties of the resonances, including the spacing distribution of the resonance positions and the distribution of the resonance widths.

(3) Statistical properties of the wave function, which is excited inside the cavity by a wave incoming through the waveguide.

We assume that the whole device consists of two different parts. The first part includes ideal leads (waveguides) which couple the device to the measuring apparatus and/or serve as a power

0022-2488/96/37(10)/4888/16/$10.00

supply. The electron/wave moves freely inside these leads, i.e., without scattering by impurities, etc. The second part contains the ''randomizing'' part of the device. Inside this part the electron acquires chaotic features, for instance, through multiple scattering on the boundary of the sample and/or impurities. We shall assume that the dynamics inside this part of the system is chaotic so that its Hamiltonian can be considered as a member of an appropriate random matrix ensemble. We shall also investigate integrable cavities (like a rectangular resonator) and show that the wave transport through it also acquires chaotic features since by connecting such a system to continua one destroys integrability. In the integrable case we shall assume that the internal Hamiltonian is described by a Poisson ensemble.

II. THE MODEL

In this section we shall construct a Hamiltonian describing a resonator coupled to waveguides. Starting with the description of the leads we assume these to support M open channels which are described by one-dimensional Hamiltonians

$$H_l = -\frac{d^2}{dx^2} + \lambda_l, \quad l = 1,\ldots,M. \tag{1}$$

Here λ_l is the threshold energy of the lth channel. Combining these operators into a Hamiltonian H_{ex} for the ''external'' part of the system, i.e., the leads, we get

$$H_{\mathrm{ex}} = -\bigoplus_{l=1}^{M} \frac{d^2}{dx_l^2} + \Lambda. \tag{2}$$

Here Λ is a diagonal matrix describing the threshold energies of the channels,

$$\Lambda = \mathrm{diag}(\lambda_1, \lambda_2, \ldots, \lambda_M). \tag{3}$$

The resonator is described by a Hermitian matrix H_{in} of size $N \times N$, with N much larger than the number of open channels, $N \gg M$. The matrix H_{in} is assumed to belong to the Gaussian orthogonal/unitary ensemble (GOE/GUE) for chaotic resonators and to a Poisson ensemble for integrable ones (see, e.g., Ref. 7 for these concepts). To describe the scattering we couple the resonator and leads by defining the Hamiltonian H of the whole system as

$$H\begin{pmatrix} u \\ u_{\mathrm{in}} \end{pmatrix} = \begin{pmatrix} H_{\mathrm{ex}} u \\ H_{\mathrm{in}} u_{\mathrm{in}} + A u'(0) \end{pmatrix}, \tag{4}$$

where $u = (u_1, \ldots, u_M)$ stands for the wave function inside the leads and u_{in} describes the wave function within the resonator; $u'(0)$ denotes the derivative of the wave functions of the leads at the points of contact with the resonator which are taken as the zeros of the waveguide coordinates, and A is an $N \times M$ coupling matrix. The local character of the coupling in Eq. (4) (a point contact) is justified whenever the diameter of the junction of lead and resonator is smaller than a typical wavelength inside the resonator. The differential operator H_{ex} can be defined on the Sobolev space $W_2^2(R_+, C^M)$ of all complex vector valued square integrable functions on R_+ having two generalized square integrable derivatives. Then the operator H is defined in the Hilbert space $\mathscr{H} = L^2(R^+, C^M) \oplus C^N$ with the scalar product

$$(U, V) = \int_0^\infty \langle u(x), v(x) \rangle_{C^M} dx + \langle u_{\mathrm{in}}, v_{\mathrm{in}} \rangle_{C^N},$$

$\langle \cdot, \cdot \rangle_{C^N}$ denotes the scalar product in the N-dimensional Hilbert space. The domain of the operator H should contain the domain $W_2^2(R_+, C^M) \oplus C^N$ but H is not self-adjoint on the latter domain.

Theorem 1: The operator H defined by formula (4) is self-adjoint on the domain of functions from $W_2^2(R_+,C^M)\oplus C^N$ satisfying the boundary conditions

$$A^\dagger u_{\rm in}=-u(0). \tag{5}$$

Proof: The boundary form of the linear operator H evaluated on the functions $U,V\in W_2^2(R_+,C^M)\oplus C^N$ is given by the following expression

$$\begin{aligned} b[U,V]&=(U,HV)-(HU,V)\\ &=\int_0^\infty \left\langle u(x),-\frac{d^2}{dx^2}\,v(x)+\Lambda v(x)\right\rangle_{C^M} dx+\langle u_{\rm in},H_{\rm in}v_{\rm in}\rangle_{C^N}\\ &\quad+\langle u_{\rm in},Av'(0)\rangle_{C^N}-\int_0^\infty \left\langle -\frac{d^2}{dx^2}\,u(x)+\Lambda u(x),v(x)\right\rangle_{C^M} dx-\langle H_{\rm in}u_{\rm in},v_{\rm in}\rangle_{C^N}\\ &\quad-\langle Au'(0),v_{\rm in}\rangle_{C^N}\\ &=\langle u(0),v'(0)\rangle_{C^M}-\langle u'(0),v(0)\rangle_{C^M}+\langle u_{\rm in},Av'(0)\rangle_{C^N}\\ &\quad-\langle Au'(0),v_{\rm in}\rangle_{C^N}. \end{aligned} \tag{6}$$

The boundary form vanishes if both elements U, V satisfy the boundary conditions (5)

$$\begin{aligned} b[U,V]&=\langle u(0),v'(0)\rangle_{C^M}-\langle u'(0),v(0)\rangle_{C^M}+\langle A^\dagger u_{\rm in},v'(0)\rangle_{C^N}-\langle u'(0),A^\dagger v_{\rm in}\rangle_{C^N}\\ &=\langle u(0),v'(0)\rangle_{C^M}-\langle u'(0),v(0)\rangle_{C^M}-\langle u(0),v'(0)\rangle_{C^M}+\langle u'(0),v(0)\rangle_{C^M}\\ &=0, \end{aligned}$$

where the dagger denotes the adjoint of an operator. This proves that the operator H is symmetric. The self-adjointness of the operator follows from the fact that the range of $H-i$ coincides with the whole Hilbert space $\mathscr{H}$. □

Note: In what follows we shall denote by H the self-adjoint operator defined by formula (4) and the boundary condition (5). The domain of the operator will be denoted by $D(H)$.

Similar models were suggested first in Refs. 8–11. Their main appeal is that they allow for a spectral analysis of the operator H in terms of elementary functions. Moreover, by calculating the eigenfunctions pertaining to the continuous spectrum one may obtain the scattering matrix in terms of the internal Hamiltonian $H_{\rm in}$ and the coupling matrix A. The eigenfunctions

$$\Psi(E)=\begin{pmatrix}\psi(E,x)\\ \psi_{\rm in}\end{pmatrix}$$

corresponding to the energy E solve the equations

$$\begin{pmatrix}-\dfrac{d^2}{dx^2}\,\psi(E,x)+\Lambda\psi(E,x)\\ H_{\rm in}\psi_{\rm in}(E)+A\psi'(E,0)\end{pmatrix}=E\begin{pmatrix}\psi(E,x)\\ \psi_{\rm in}\end{pmatrix}. \tag{7}$$

The second of the foregoing equations leads, together with the boundary condition (5), to the following energy-dependent condition for the external component of the wave function,

$$\psi(E,0)=A^\dagger\,\frac{1}{H_{\rm in}-E}\,A\psi'(E,0). \tag{8}$$

Moreover, the external component is a solution of the free Schrödinger equation. For the energy $E \neq \lambda_j$, $j=1,\ldots,M$, it can be presented in the form

$$\psi(E,x)=\frac{e^{-i\sqrt{E-\Lambda}x}}{\sqrt[4]{E-\Lambda}}\mathscr{A}_{\text{inc}}-\frac{e^{i\sqrt{E-\Lambda}x}}{\sqrt[4]{E-\Lambda}}\mathscr{A}_{\text{out}}, \tag{9}$$

where $\mathscr{A}_{\text{inc}}$ and $\mathscr{A}_{\text{out}}$ are the amplitudes of the incoming and outgoing wave, respectively. For all $E>\max\{\lambda_j\}$ every solution is bounded and the scattering matrix $S(E)$ can easily be defined. The normalization used in Eq. (9) ensures that the S-matrix relates the amplitudes of the incoming and outgoing waves as

$$\mathscr{A}_{\text{out}}=S(E).\mathscr{A}_{\text{inc}}.$$

The scattering matrix can be calculated substituting the external component of the wave function into the energy-dependent boundary condition (8). The boundary values of the external component at the ''origin,'' i.e., at the coupling points, are equal to

$$\psi(0)=Q(1-S).\mathscr{A}_{\text{inc}}, \quad \psi'(0)=iQ^{-1}(-1-S).\mathscr{A}_{\text{inc}},$$

where $Q\equiv Q(E)$ denotes the $M\times M$ matrix $Q(E)=(E-\Lambda)^{-1/4}$. For energies above the thresholds the S-matrix can be determined through the following:

Lemma 1: The stationary scattering matrix for the operator H is equal to

$$S(E)=\frac{i+\widetilde{W}^{\dagger}(E-H_{\text{in}})^{-1}\widetilde{W}}{i-\widetilde{W}^{\dagger}(E-H_{\text{in}})^{-1}\widetilde{W}}, \tag{10}$$

where $E>\max\{\lambda_j\}$ and $\widetilde{W}=AQ^{-1}$.

Similar results were obtained earlier in Ref. 11.

The knowledge of the Hamiltonian of the system enables us to go beyond the standard scattering characteristics and to solve Eq. (7) for the internal-component of the wave function,

$$\psi_{\text{in}}=\frac{2}{E-H_{\text{in}}}\widetilde{W}\frac{1}{i-\widetilde{W}^{\dagger}(E-H_{\text{in}})^{-1}\widetilde{W}}\mathscr{A}_{\text{inc}}. \tag{11}$$

In Sec. IV we shall use this formula to evaluate the structure of the wave function in the internal (interaction) part of the system.

Before proceeding further let us shortly comment on the properties of the S-matrix (10). First, we show that the S-matrix (10) can be rewritten in the more familiar form[12]

$$S=I-2\pi i W^{\dagger}\frac{1}{E-H_{\text{in}}+i\pi WW^{\dagger}}W. \tag{12}$$

To prove the equivalence of Eqs. (10) and (12) we use the resolvent equation

$$R(E)=R_0(E)-i\pi R_0(E)P[1+i\pi PR_0(E)P]^{-1}PR_0(E) \tag{13}$$

with $R(E)=(E-H_{\text{in}}+i\pi WW^{\dagger})^{-1}$, $R_0(E)=(E-H_{\text{in}})^{-1}$, and $P=WW^{\dagger}$. Inserting this into Eq. (12) we obtain after a simple calculation

$$S=\frac{i+\pi W^{\dagger}R_0(E)W}{i-\pi W^{\dagger}R_0(E)W},$$

which is fully equivalent to Eq. (10) provided we identify $\widetilde{W}$ and $\sqrt{\pi}W$. There is, however, one important difference: The coupling matrix $\widetilde{W}$ is energy dependent. This dependence takes into account the threshold effects which are often disregarded in the stochastic approach; it has, however, measurable consequences and leads to the correct high-energy behavior of the S-matrix.[13] We shall come back to this point in Sec. V when we use the model to describe the experimental results obtained for rectangular electromagnetic resonators.

III. RESONANCE DISTRIBUTION

We now propose to study how the distribution of nearest-neighbor spacings between the resonances of our open system differs from the distribution of spacings between eigenenergies of the closed resonator. For simplicity we confine ourselves to the simplest case, that of a single open channel, $M=1$. The original $N\times M$ matrix A becomes then an N-component vector. We shall focus on an integrable resonator rather than a chaotic one since in this case the differences in question turn out to be most drastic: roughly speaking, the opening of the resonator by waveguides destroys the usual spectral signatures of integrability. In what follows we assume that the coupling vector A is normalized as

$$A=ga, \quad \|a\|=1,$$

and that the coupling constant g is large, $g\gg 1$. The resonances of the whole system are the eigenvalues of the effective ''Hamiltonian''

$$H_{\text{eff}}=H_{\text{in}}-i\widetilde{W}\widetilde{W}^{\dagger}=H_{\text{in}}-ig^2aQ^2a^{\dagger}.$$

The ''perturbation'' $-i\widetilde{W}\widetilde{W}^{\dagger}$ of H_{in} is negative imaginary and has rank one. Every eigenfunction of the effective Hamiltonian H_{eff} is a solution to the equation

$$(H_{\text{in}}-ig^2aQ^2a^{\dagger})\psi_{\text{in}}=E\psi_{\text{in}},$$

and comes with a certain resonance energy $E\in\mathbb{C}$. Applying the resolvent of the internal Hamiltonian to the latter equality we get a ''dispersion equation'' for the resonance energy,

$$\frac{1}{g^2\sqrt{\lambda-E}}=a^{\dagger}\,\frac{1}{H_{\text{in}}-E}\,a. \tag{14}$$

Denoting by $F(E)$ the right-hand side (rhs) of Eq. (14) and expressing it in the eigenrepresentation of H_{in} we have

$$F(E)=\sum_{n=1}^{N}\frac{|a_n|^2}{E_n-E}, \tag{15}$$

where E_n are the eigenvalues of the internal Hamiltonian. The function $F(E)$ has a positive imaginary part in the upper half plane and is real on the real axis. Therefore all solutions of Eq. (14) are localized in the lower complex half plane. Consider the case of strong coupling, $g\to\infty$. Then all solutions of the dispersion equation (14) are situated at the zeros of the function $F(E)$. Our aim here is to investigate the distribution of spacings between such zeros (following a method similar to that used in Ref. 14).

It is clear that between two poles there is exactly one zero of $F(E)$. Moreover, two neighboring zeros are locked between three neighboring poles. Since we are interested in the distribution of resonance spacings for small spacings, it suffices to restrict the sum $F(E)$ in Eq. (15) to three terms only, namely, to those whose poles lock up the two colliding zeros of $F(E)$. Let us

label those poles by E_1, E_2, E_3. In order to simplify the expressions (but without loss of generality) we shift the origin of the energy scale to the central pole such that $E_2=0$, whereupon E_1 is negative, $E_1<0$. Then the eigenvalue equation (14) simplifies to

$$\frac{w_1}{E_1-E}-\frac{w_2}{E}+\frac{w_3}{E_3-E}=0 \tag{16}$$

with $w_i=|a_i|^2$, $i=1,2,3$. The two zeros in discussion solve the quadratic equation

$$(w_1+w_2+w_3)E^2-[(w_1+w_2)E_3+(w_2+w_3)E_1]E+w_2E_1E_3=0, \tag{17}$$

and their squared distance $D=s^2$ is given by

$$D=\frac{[(w_1+w_2)E_3+(w_2+w_3)E_1]^2}{(w_1+w_2+w_3)^2}-\frac{w_2E_1E_3}{w_1+w_2+w_3}. \tag{18}$$

Our aim here is to investigate the cumulative probability of these squared spacings, $P(D)=P((z_1-z_2)^2\leqslant D)$, where z_1 and z_2 are the two solutions of Eq. (17) in the case when the internal Hamiltonian H_{in} belongs to the Poisson ensemble, i.e., corresponds to an integrable system. As already announced above that distribution will reveal level repulsion due to the attached waveguides, even though the internal Hamiltonian H_{in} belongs to the Poisson ensemble, i.e., corresponds to an integrable system. Before proceeding further we shall need the following.

Lemma 2: (a) $f(t)\equiv t^\alpha \exp(-t)\leqslant a^\alpha e^{-\alpha}\ \forall t\geqslant 0$, $\alpha>0$. (b) Let $0<\alpha<1$, $b>0$; *then the following estimate is valid*:

$$\int_0^\infty \frac{e^{-br}}{r^{1-\alpha}}\,dr\leqslant \frac{1}{\alpha}+\frac{1}{b}.$$

Proof: (a) holds because f is continuous with maximum at $t=\alpha$. (b) follows from

$$\int_0^\infty \frac{e^{-br}}{r^{1-\alpha}}\,dr=\int_0^1 \frac{e^{-br}}{r^{1-\alpha}}\,dr+\int_1^\infty \frac{e^{-br}}{r^{1-\alpha}}\,dr\leqslant \int_0^1 \frac{1}{r^{1-\alpha}}\,dr+\int_1^\infty e^{-br}dr\leqslant \frac{1}{\alpha}+\frac{1}{b}.$$

□

A. Estimates from above

It follows from Eq. (18) that one can use the following lower estimate for D,

$$D\geqslant -4\,\frac{w_2}{w_1+w_2+w_3}\,E_1E_3. \tag{19}$$

This inequality implies

$$P(D)\leqslant P(X) \tag{20}$$

with $X=-4[w_2/(w_1+w_2+w_3)]E_1E_3$.

Case 1. Constant coupling $w_1=w_2=w_3=1$

Let us assume first that the coefficients w_i are constant and equal, as is not unreasonable when the antenna is attached to a ''symmetry point'' of the resonator and when we restrict ourselves to resonances belonging to one parity class only. For a rectangular resonator this means that we couple the antenna to the geometric center and investigate only resonances which have even–even parity. The probability can be estimated as follows,

$$P(D) \leqslant \int_0^D da \int_{-\infty}^0 dE_1 e^{E_1} \int_0^\infty dE_3 e^{-E_3} \delta(-\tfrac{4}{3}E_1E_3 - a)$$

$$= -\int_0^D da \int_{-\infty}^0 dE_1 \frac{3}{4E_1} \exp(E_1) \exp\left\{\frac{3a}{4E_1}\right\}.$$

Thus for any $0<\alpha<1$ we have using Lemmas 2 and 3

$$P(D) \leqslant -\int_0^D da \frac{3}{4} \int_{-\infty}^0 dE_1 \frac{e^{E_1}}{E_1} \left(-\frac{3a}{4E_1}\right)^{-\alpha} \left(-\frac{3a}{4E_1}\right)^{\alpha} \exp\left\{\frac{3a}{4E_1}\right\}$$

$$\leqslant \left(\frac{3}{4}\right)^{1-\alpha} \int_0^D da \frac{\alpha^\alpha}{a^\alpha} \left(1+\frac{1}{\alpha}\right) e^{-\alpha}$$

$$= \left(\frac{3}{4}\right)^{1-\alpha} \frac{\alpha^\alpha}{1-\alpha} \left(1+\frac{1}{\alpha}\right) e^{-\alpha} D^{1-\alpha}$$

$$= C_1(\alpha) D^{1-\alpha}.$$

We note that the latter estimate is valid for any positive value of the parameter α, but the constant $C_1(\alpha)$ tends to infinity when α tends to zero.

Case 2. Poisson distribution of w_i

Another physically relevant case we discuss here is the case when the coupling vector a is complex with coefficients whose real and imaginary parts are independent and normally distributed. Then the w_i are independent random numbers with a χ^2 distribution with two degrees of freedom. Moreover, the sum $w_1+w_2+w_3$ has a χ^2 distribution with 6 degrees of freedom. Having this in mind we obtain that $y=w_2/(w_1+w_2+w_3)$ has a distribution with a density given by $p(y)=2(1-y)$, $y\in[0,1]$. Using Lemma 2 we can estimate $P(D)$ as follows, given by

$$P(D) \leqslant \int_0^D da \int_{-\infty}^0 dE_1 e^{E_1} \int_0^\infty dE_3 e^{-E_3} \int_0^1 dy 2(1-y) \delta(-4yE_1E_3 - a)$$

$$= -\int_0^D da \int_{-\infty}^0 dE_1 e^{E_1} \int_0^1 dy e^{a/4yE_1} \frac{1}{4yE_1} 2(1-y)$$

$$= \int_0^D \frac{da}{a^\alpha} \int_{-\infty}^0 dE_1 e^{E_1} \int_0^1 dy e^{a/4yE_1} \left(-\frac{1}{4yE_1}\right)^{1-\alpha} \left(-\frac{a}{4yE_1}\right)^{\alpha} 2(1-y)$$

$$\leqslant \int_0^D \frac{da}{a^\alpha} \int_0^1 dy 2(1-y) \frac{\alpha^\alpha e^{-\alpha}}{(4y)^{1-\alpha}} \left(\frac{1}{\alpha}+1\right) \leqslant C_2(\alpha) D^{1-\alpha}$$

for any $1>\alpha>0$. Similarly as in the previous case $C_2(\alpha)$ is some function of α with $\lim_{\alpha\to 0} C_2(\alpha)=\infty$. Thus we got the same estimate as in the case 1.

A similar estimate is also valid in the case where the components of the vector w are real independent random numbers equally distributed in the interval $[0,1]$.

B. Lower estimates

To obtain a lower estimate for $P(D)$ we use first following upper estimate for the distance between the two zeros:

$$(z_1-z_2)^2 \leqslant (-E_1+E_3)^2.$$

Then

$$P(D) \geqslant \int_0^D da \int_{-\infty}^0 dE_1 e^{E_1} \int_0^\infty dE_3 e^{-E_3} \delta((-E_1+E_3)^2-a)$$

$$= \int\int_{-E_1+E_3 \leqslant \sqrt{D}} dE_1 dE_3 e^{-(-E_1+E_3)}$$

$$= \frac{1}{2} \int_0^{\sqrt{D}} dx e^{-x} \int_{-x}^{x} dy$$

$$= \int_0^{\sqrt{D}} dx e^{-x} x = 1 - e^{-\sqrt{D}}(1+\sqrt{D}).$$

Thus the probability $P(D)$ can be approximated from below by a linear function for small values of D,

$$P(D) \geqslant D + o(D) \geqslant BD,$$

where $B \leqslant 1$, $o(D)/D \to 0$ as $D \to 0$.

C. Asymptotic behavior at small spacings

Combining together lower and upper estimates for the probability we can write

$$BD \leqslant P(D) \leqslant C(\alpha) D^{1-\alpha}. \tag{21}$$

A similar estimate can be obtained also for the probability of resonance spacings $\tilde{P}(s)$, $s^2 = D$:

$$Bs^2 \leqslant \tilde{P}(s) \leqslant C(\alpha) s^{2-2\alpha}. \tag{22}$$

The physically relevant quantity is, however, not the distribution $\tilde{P}(s)$ but the corresponding probability density $p(s)$:

$$\tilde{P}(s) = \int_0^s p(t) dt.$$

Suppose that for small s the probability density has the behavior

$$p(s) \sim k s^\beta + o(s^\beta),$$

with some real constants k and β. Substituting the last asymptotic expansion into the estimate (22) we get for the constants k and β

$$\beta = 1, \quad k \geqslant 2B.$$

It follows that the probability density of the spacing s is approximately linear for small values of s. This estimate shows that the presence of the antenna changes the character of the resonance spacing distribution from Poisson to a distribution which displays linear repulsion for small s. For the slope k of the distribution we find $k \geqslant 2$ for small s. This means that the slope k is always larger than the slope of the spacing probability density in a fully chaotic system, which is given by the Wigner distribution with a slope equal to $\pi/2$. The resonance repulsion is therefore always weaker than the level repulsion for a typical GOE matrix.

IV. INTERNAL WAVE FUNCTION

Let us now discuss the properties of the internal wave function (11). To investigate the structure of ψ_{in} in a more detailed way we introduce a coupling constant g and will write $g\tilde{W}$ for the coupling matrix. The complicated part of this expression is contained in the term

$$\frac{1}{i-g^2T(E)} \tag{23}$$

with the $M\times M$ matrix $T(E)=\tilde{W}^{\dagger}(E-H_{\text{in}})^{-1}\tilde{W}$. We solve the spectral problem for the latter matrix:

$$T(E)f_n=\lambda_n(E)f_n \tag{24}$$

[note that for E real $T(E)$ is a symmetric matrix and hence the eigenvalues $\lambda_n(E)$ are real numbers] and use the eigenvectors f_n to define the M vectors ψ_n living in the N-dimensional internal space:

$$\psi_n=(E-H_{\text{in}})^{-1}\tilde{W}f_n\,. \tag{25}$$

(We shall normalize the vectors f_n, so that $\|f_n\|=1$. This means that the vectors ψ_n are not normalized.)

The vector ψ_n is a solution of the equation

$$\left(H_{\text{in}}+\frac{1}{\lambda_n(E)}\,\tilde{W}\tilde{W}^{\dagger}\right)\psi_n=E\psi_n\,. \tag{26}$$

To reveal the usefulness of these vectors we employ the spectral decomposition of the operator (23):

$$\frac{1}{i-g^2T(E)}=\sum_{n=1}^{M}\;\frac{f_nf_n^{\dagger}}{i-g^2\lambda_n(E)} \tag{27}$$

(where $f_nf_n^{\dagger}$ is the projector onto the one-dimensional subspace spanned by the vector f_n). Inserting this into the internal wave function (11) we finally obtain

$$\psi_{\text{in}}=2g\sum_{n=1}^{M}\;\frac{\langle f_n\,,\mathscr{A}_{\text{inc}}\rangle_{C^M}}{i-g^2\lambda_n(E)}\;\psi_n\,. \tag{28}$$

It is most interesting to realize, thus, that internal wave functions (each with N components) can be linearly composed from only M (fewer!) N-component vectors ψ_n.

It can be easily seen that for real energies E the vectors ψ_n are real provided H_{in} and $\tilde{W}$ are real matrices. The properties of the internal wave function ψ_{in} depend substantially on the structure of these vectors and on the number of terms which contribute to the sum (28). In what follows we shall investigate the structure of ψ_{in} for resonances.

Resonances are defined as poles of the S-matrix in the complex energy plane. Using the above notation the resonances $E_{\text{reson}}=E_r-i\Gamma$ are nothing but the solutions of the following sequence of equations:

$$\lambda_n(E_{\text{reson}})=\frac{i}{g^2},\quad n=1,\ldots,M. \tag{29}$$

(E_r describes the position of the resonance peak, while Γ gives its width.) We shall now assume that the energy E in the incoming wave coincides with the position of some resonance: $E=E_r$. To obtain information about $\psi_{\rm in}$ we insert Eq. (29) into Eq. (26) obtaining for ψ_n

$$(H_{\rm in}-ig^2\tilde{W}\tilde{W}^{\dagger})\psi_n=E_{\rm reson}\psi_n\,. \tag{30}$$

It follows therefore that in the resonance case ψ_n are identical with the eigenvectors of the effective Hamiltonian $H_{\rm eff}=H_{\rm in}-ig^2\tilde{W}\tilde{W}^{\dagger}$.

For weak coupling ($g\ll 1$) the resonances are localized near the eigenvalues of $H_{\rm in}$ and the resonance widths are small ($\Gamma\ll 1$). Moreover, it follows from Eq. (30) that the vectors ψ_n practically coincide with the eigenvectors of $H_{\rm in}$. Using the relation $i-g^2\lambda_n(E_r)=-ig^2\Gamma\Lambda_n'(E_r)+O(g^4)$ we obtain from Eq. (28)

$$\psi_{\rm in}=2i\,\frac{\langle f_{n_0}|\mathscr{A}_{\rm inc}\rangle_{C^M}}{g\Gamma\lambda_n'(E_r)}\,\psi_{n_0}+O(g)\,, \tag{31}$$

where ψ_{n_0} refers to the appropriate solution of Eq. (30). Consequently, the structure of $\psi_{\rm in}$ coincides with the structure of ψ_{n_0}, which is [up to terms of the order $O(g)$] identical with the corresponding eigenvector of $H_{\rm in}$.

A similar analysis can be done also for strong coupling ($g\gg 1$). Since $\tilde{W}\tilde{W}^{\dagger}$ is a matrix of rank M the family of resonances can be split into two parts: M resonances are localized deep in the lower complex half plane and have widths $\Gamma\approx g^2$, and the remaining $N-M$ resonances approach the real axis and have widths $\Gamma\approx 1/g^2$. We are interested in the second group of resonances, since they form sharp resonance peaks and are hence easily measurable. A similar analysis as in the weak coupling case gives

$$\psi_{\rm in}=2i\,\frac{\langle f_{n_0}|\mathscr{A}_{\rm inc}\rangle_{C^M}}{g\Gamma\lambda_n'(E_r)}\,\psi_{n_0}+O\left(\frac{1}{g}\right). \tag{32}$$

This formula seems to be nearly the same as for weak coupling. There is, however, one deep difference: the position of the resonance E_r does not tend as $g\to\infty$ to some eigenvalue of the internal Hamiltonian $H_{\rm in}$. This in turn means that the corresponding vector ψ_{n_0} does not coincide with an eigenvector of $H_{\rm in}$. In fact, for a generic coupling matrix W the vector ψ_{n_0} is a real superposition of all eigenvectors of $H_{\rm in}$.

For intermediate coupling the resonances overlap and one has to take all terms in Eq. (28) into account. $\psi_{\rm in}$ is in this case a superposition of the vectors ψ_n with complex coefficients.

Let us now discuss the consequences of the above analysis for the statistical properties of the internal wave function $\psi_{\rm in}$. For weak coupling the properties of $\psi_{\rm in}$ coincide with those of the corresponding eigenfunction of $H_{\rm in}$. This means that in the GOE case $|\psi_{\rm in}|^2$ has a Porter–Thomas distribution, similarly for strong coupling. In this case $\psi_{\rm in}$ is proportional to a *real* superposition of the eigenvectors of $H_{\rm in}$. This means again a Porter–Thomas distribution in the GOE case.

The structure of $\psi_{\rm in}$ becomes interesting in particular for $H_{\rm in}$ describing an integrable system. We know that $\psi_{\rm in}$ becomes a *superposition* of the (integrable) eigenvectors of $H_{\rm in}$. Hence the internal wave function acquires a structure other than an eigenvector of integrable system. We shall show in the next section that $\psi_{\rm in}$ has features which are similar to the properties of eigenvectors of chaotic quantum systems. This fact supports the finding of the preceding section that opening an integrable system leads to a level repulsion which is typical for the behavior of quantum nonintegrable systems.

It remains to discuss the moderate-coupling case. Here, as already mentioned, the internal vector $\psi_{\rm in}$ becomes a superposition of vectors ψ_n with *complex* coefficients. The consequence is that the statistical properties of $\psi_{\rm in}$ differ from the standard predictions of the random-matrix

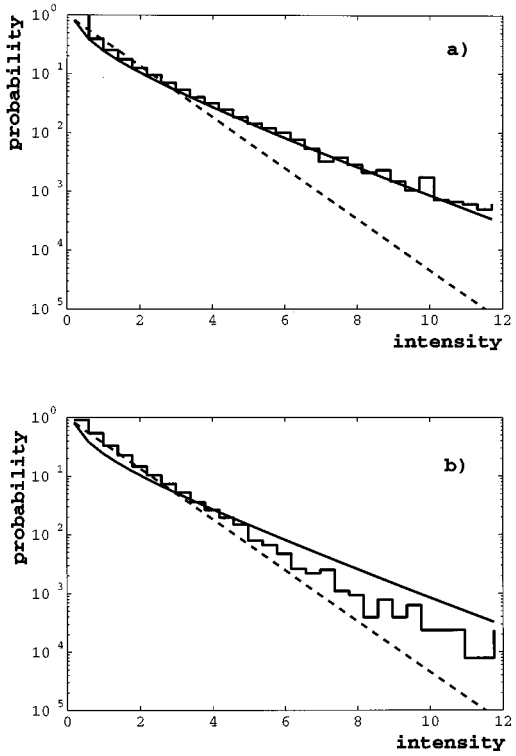

FIG. 1. The intensity distribution $|\psi|^2$ of the internal wave function (11) excited inside the resonator cavity is plotted in a semilogarithmic plot and compared with the Porter–Thomas (dashed line) and the Poisson (Rayleigh) distribution (full line). (a) pertains to one open channel ($M=1$). Good agreement with the Porter–Thomas distribution is visible. (b) shows the result for $M=10$ with a clear shift towards the Poisson distribution.

theory. The complex nature of ψ_{in} moves its statistical properties from a GOE prediction (Porter–Thomas distribution) toward a GUE prediction (Poisson distribution). (Note that ψ_{in} will display a Poisson distribution if its real and imaginary parts are statistically independent and of the same magnitude.) Such a distribution (also known as Rayleigh distribution in the literature[15]) is usually observed when waves excited by a monochromatic source propagate through a random medium—see also Ref. 16. In our case the randomizing effect is due solely to the multiple reflection of the waves inside the resonator. Numerical estimates show that already for $M=3$ the Rayleigh intensity pattern inside the resonator is well developed (see Fig. 1).

V. EXAMPLE

Let us now discuss a rectangular resonator attached to two microwave cables each of which supports one open channel. We assume that the channel threshold energies are set to zero, $\lambda_1=\lambda_2=0$. This system has recently been experimentally investigated in Refs. 4, 5, and 17. The Hamiltonian H_{reson} describing the resonator is given by the two-dimensional Laplace operator

$$H_{\text{reson}}=-\Delta$$

defined on a bounded domain Ω with Dirichlet boundary conditions $f=0$ on the boundary $\partial\Omega$. We shall investigate the statistical properties of the resonances and the structure of the field intensity inside the resonator as excited by waves entering through the microwave cable. Let E_n $[f_n(\mathbf{r}),\mathbf{r}\in\mathbb{R}^2]$ be the eigenvalues [eigenfunctions] of H_{reson}:

$$H_{\text{reson}} f_n(\mathbf{r}) = E_n f_n(\mathbf{r}). \tag{33}$$

Using these solutions let us define the finite-dimensional internal Hamiltonian acting on the space spanned by the first N eigenstates of H_{reson},

$$H_{\text{in}} = \sum_{n=1}^{N} E_n f_n f_n^{\dagger}. \tag{34}$$

The coupling operator A maps the two-dimensional vector

$$\begin{pmatrix} u_1'(0) \\ u_2'(0) \end{pmatrix}$$

into a certain function belonging to the N-dimensional internal space. Let $u_1(x)$ $[u_2(x)]$ denote the first, [second] component of the wave function in the cable. Applying the matrix A to the incoming vector we get

$$A\begin{pmatrix} u_1'(0) \\ u_2'(0) \end{pmatrix} = \alpha_1 d_1^N(\mathbf{r}) u_1'(0) + \alpha_2 d_2^N(\mathbf{r}) u_2'(0),$$

where α_1 and α_2 are the coupling constants and d_l^N, $l=1,2$ are functions spanned by the vectors f_n, $n=1,\ldots,N$. In the experiment the two antennas are coupled to the resonator at the points $\mathbf{r}_1$ and $\mathbf{r}_2$. In order to mimic this local coupling we choose the functions $d_l^N(\mathbf{r})$, $l=1,2$, in a special way, namely, such that they converge to $\delta^2(\mathbf{r}-\mathbf{r}_l)$ when $N\to\infty$, i.e.,

$$d_l^N(\mathbf{r}) = \sum_{i=1}^{N} f_i(\mathbf{r}_l) f_i(\mathbf{r}) \tag{35}$$

such that $\lim_{N\to\infty} d_l^N(\mathbf{r}) = \delta^2(\mathbf{r}-\mathbf{r}_l)$ (in the sense of generalized functions with $\mathbf{r}\in\mathbb{R}^2$).

The Hamiltonian H describing the whole system is self-adjoint on the domain determined by the boundary conditions

$$\langle d_l^N, u_{\text{in}} \rangle = -u_l(0).$$

In the limit $N\to\infty$ the boundary conditions are given by the formula

$$\alpha_l u_{\text{in}}(\mathbf{r}_l) = -u_l(0).$$

For N large enough the S-matrix reads

$$S = \frac{i + T(E)}{i - T(E)} \tag{36}$$

where $T(E)$ is a 2×2 matrix with elements

$$T(E)_{l,m} = \alpha_l \alpha_m \sqrt{E} \sum_{n=1}^{N} \frac{f_n(\mathbf{r}_l) f_m(\mathbf{r}_m)}{E_n - E}. \tag{37}$$

(Implicitly a similar formula has already been used in Ref. 18 in order to evaluate the conductance fluctuation for electrons passing a quantum dot.)

Let us start with the simplest case with one attached antenna only. (The second antenna is easily excluded by choosing the coupling $\alpha_2=0$.) In what follows we shall focus on the statistical properties of the resonances inside such a resonator.

The resonances are identified with the poles of the corresponding S-matrix. In the case of one coupled antenna the resonances are just the solutions of the algebraic equation $T(E)=i$, which is equivalent to

$$\sum_{n=1}^{N} \frac{|f_n(\mathbf{r}_1)|^2}{E_n-E} = \frac{i}{\alpha_1^2\sqrt{E}}. \tag{38}$$

This is an algebraic equation for E which has solutions on the lower complex half plane only. The solutions coincide with the zeros of a certain polynomial of order $2N+1$. One can solve this equation directly using some appropriate numerical method. But before doing this it seems to be helpful to investigate this equation by decoupling it into real and imaginary parts. Let $E=E_r-i\Gamma$ denote a solution with E_r and Γ the position and the width of the resonance, respectively. Assuming that $\Gamma \ll E_r$ we can approximate Eq. (38) by

$$\sum_{n=1}^{N} \frac{|f_n(\mathbf{r}_1)|^2}{E_n-E_r} = 0, \tag{39}$$

whereby the corresponding resonance widths are given by

$$\Gamma = 1 \Big/ \alpha_1^2\sqrt{E_r}\sum_{n=1}^{N} \frac{|f_n(\mathbf{r}_1)|^2}{(E_n-E_r)^2}. \tag{40}$$

This approximation is well justified in particular in the case of strong coupling ($\alpha_1 \gg 1$). In the numerical tests we used this approximate solution as a starting point for a routine searching for the complex roots of Eq. (38).

For the wave function ψ excited inside the resonator we find

$$\psi(\mathbf{r}) = \sum_{k=1}^{2}\sum_{l=1}^{2} 2(E)^{1/4}\alpha_k G(\mathbf{r},\mathbf{r}_k,E)\left(\frac{1}{i-T(E)}\right)_{k,l} \mathscr{A}_{\mathrm{inc},l}, \tag{41}$$

where

$$G(\mathbf{x},\mathbf{x}_k,E) = \sum_{n=1}^{N} \frac{f_n(\mathbf{x})\overline{f_n(\mathbf{x}_k)}}{E_n-E}$$

and $\mathscr{A}_{\mathrm{inc},l}$ denotes the amplitude of the incoming wave in the channel l. It is clear that in the case of a strong coupling to the antenna the structure of the resonance wave function differs substantially from the structure of the original resonator eigenfunction $f_n(x)$.

Let us now apply the above theory to the description of a rectangular resonator with one attached antenna. In the case of a rectangular resonator the eigenvalues E_n and the eigenfunctions f_n are explicitly known. Inserting these solutions into the formulas above we obtain an explicit solution of the perturbed resonator problem. As already mentioned, the resonances of such a system have been measured systematically.[19] In order to enhance the number of measured resonances the results for various rectangular billiards have been combined. In order to reproduce the experimental results we have evaluated resonances for 40 different rectangular billiards. In each billiard we evaluated the first 350 resonances which roughly correspond with the number of experimentally accessible ones. The obtained results have been rescaled (to obtain a mean resonance spacing equal to 1) and divided into three groups: the first group corresponds to resonances

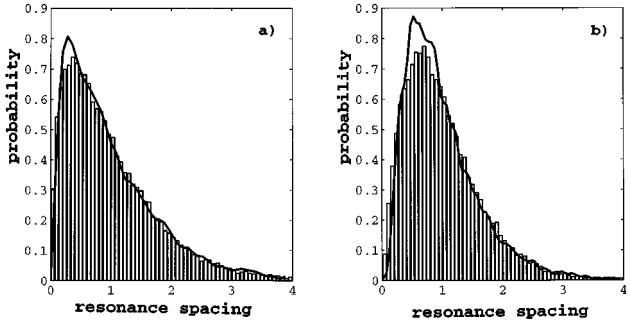

FIG. 2. The distribution of resonance spacings evaluated for a rectangular billiard is plotted (bins) and compared with the experimental results obtained in Ref. 19 (full line). The frequency range used was (a) 5–10 GHz; (b) 10–15 GHz.

measured within the frequency range 5–10 GHz, the second group corresponds to 10–15 GHz, and the third to a frequency range 15–18 GHz. The resonance spacing statistics have been evaluated for each group separately. The coupling constant α_1 has been taken to be equal to 2 in all three cases. The obtained results are plotted in Fig. 2 and compared with the experimental finding. It is worth noting that the theory predicts the effective coupling of the antenna to the resonator to become stronger for higher frequencies. This follows from the fact that the effective coupling of the antenna depends on $\alpha_1^2\sqrt{E}$ and hence on the wave frequency ω. (Note that the energy E and the microwave frequency ω are related by $E \approx \omega^2$.)

The distribution of the corresponding resonance widths is plotted in Fig. 3. We have compared this distribution with the recent prediction by Fyodorov and Sommers[20] for fully chaotic systems (resonators) with one open channel. It is interesting to remark that even though the rectangular resonator is originally integrable the distribution of resonance widths resembles closely that of a fully chaotic system. Clearly, then, the antenna represents a strong perturbation of the original integrable system. This perturbation is also responsible for the observed linear resonance repulsion visible in Fig. 2.

The influence of the antenna on the structure of the corresponding resonance function (i.e., on the structure of the electromagnetic field excited inside the resonator) is demonstrated in Fig. 4.

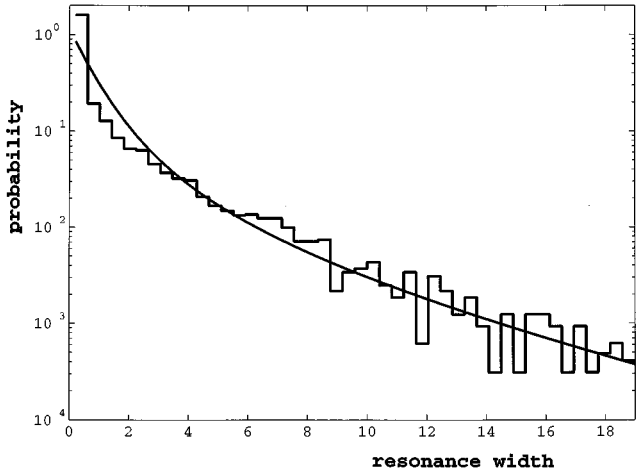

FIG. 3. The distribution of resonance widths evaluated for the frequency range 10–15 GHz is compared with the theoretical prediction for a fully chaotic system with one open channel (Ref. 20).

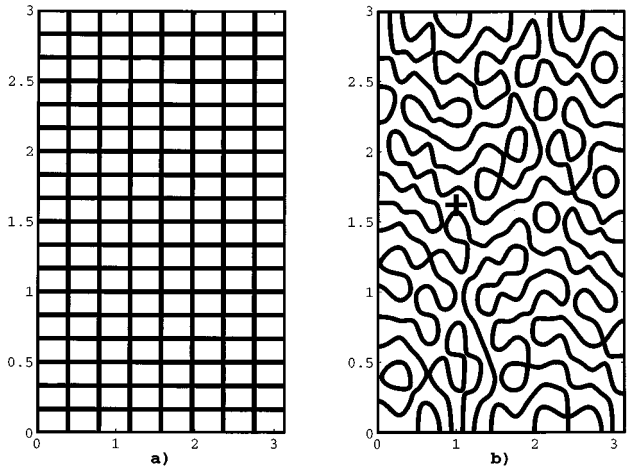

FIG. 4. Nodal lines of the electric field intensity inside a rectangular resonator with sides of lengths π and 3. (a) pertains to the unperturbed 187th state. (b) shows how this nodal line pattern changes after an antenna has been attached at the point marked by a cross.

The figure shows that the structure of the original eigenfunction f_n of the resonator is destroyed.

ACKNOWLEDGMENTS

We gratefully acknowledge support by the Deutsche Forschungsgemeinschaft through the Sonderforschungsbereich Unordnung und grosse Flukruationen. One of the authors (M.K.) was partially supported by the Polish KBN Grant No. 2 P03B 093 09. Another author (P.Š.) was partially supported by the Czech Grant No. AS CR 148409. Another author (P.K.) is grateful to the Alexander von Humboldt Foundation for the financial support.

APPENDIX: PERTURBATION OF THE NEUMANN BOUNDARY CONDITION

The interaction between the external and internal channels can be introduced in a different way. Consider, for example, the operator

$$H_B\begin{pmatrix} u \\ u_{\rm in}\end{pmatrix}=\begin{pmatrix} H_{\rm ex}u \\ H_{\rm in}u_{\rm in}+Bu(0)\end{pmatrix} \tag{A1}$$

with B being a self-adjoint operator. H_B is self-adjoint on the domain of functions from $W_2^2(R_+,C^M)\oplus C^N$ satisfying the boundary conditions

$$B^\dagger u_{\rm in}=u'(0).$$

We arrive at the following energy-dependent boundary conditions for the eigenfunctions of the operator H_B:

$$\psi'(E,0)=-B^\dagger(H_{\rm in}-E)^{-1}B\psi(E,0).$$

Then the scattering matrix above the thresholds is given by

$$S(E)=-\frac{i+\tilde{W}_B^\dagger(E-H_{\rm in})^{-1}\tilde{W}_B}{i-\tilde{W}_B^\dagger(E-H_{\rm in})^{-1}\tilde{W}_B},$$

where $\widetilde{W}_B = BQ$. For the small coupling, $\widetilde{W}_B \to 0$, the scattering matrix tends to -1 and this shows that the model operator constructed here can be considered as a perturbation of the operator H_{ex} with the Neumann boundary conditions at the origin.

[1] H. U. Baranger and P. A. Mello, Phys. Rev. Lett. **73**, 142 (1994).
[2] M. J. Berry *et al.*, Surf. Sci. **305**, 495 (1994).
[3] A. M. Chang, H. U. Baranger, L. N. Pfeiffer, and K. W. West, Phys. Rev. Lett. **73**, 2111 (1994).
[4] A. Kudrolli, S. Sridhar, A. Pandey, and R. Ramaswamy, Phys. Rev. E **49**, R11 (1994).
[5] H. J. Stoeckmann and J. Stein, Phys. Rev. Lett. **64**, 2215 (1990).
[6] Z. Pluhar, H. A. Weidenmueller, J. A. Zuk, and C. H. Levenkopf, Phys. Rev. Lett. **73**, 2115 (1994).
[7] F. Haake, *Quantum Signatures of Chaos* (Springer, Berlin, 1991).
[8] B. S. Pavlov, Teor. Mat. Fiz. **59**, 345 (1984).
[9] B. S. Pavlov, Russian Math. Surveys **42**, 127 (1987).
[10] P. B. Kurasov, Lett. Math. Phys. **25**, 287 (1992).
[11] P. B. Kurasov and B. S. Pavlov, in *On Three Levels*, edited by M. Fannes *et al.* (Plenum, New York, 1994).
[12] Z. Pluhar, H. A. Weidenmueller, J. A. Zuk, C. H. Lewenkopf, and F. J. Wegner, Ann. Phys. **243**, 1 (1995).
[13] A. M. Lane and R. G. Thomas, Rev. Mod. Phys. **30**, 257 (1958).
[14] S. Albeverio and P. Šeba, J. Stat. Phys. **64**, 369 (1991).
[15] K. J. Ebeling, in *Physical Acoustics*, edited by W. P. Mason and R. N. Thurston (Academic, New York, 1984), Vol. 17.
[16] R. Pnini and B. Shapiro, Preprint Technion, Haifa, 1996 (unpublished).
[17] U. Stoffregen, J. Stein, H. J. Stoeckmann, F. Haake, and M. Kuś, Phys. Rev. Lett. **74**, 2666 (1995).
[18] V. N. Prigodin, K. B. Efetov, and S. Iida, Phys. Rev. Lett. **71**, 1230 (1993).
[19] F. Haake, G. Lenz, P. Šeba, J. Stein, H.-J. Stoeckmann, and K. Zyczkowski, Phys. Rev. A. **44**, R6161 (1991).
[20] Y. V. Fyodorov and H-J. Sommers, Report cond-mat. No. 9507117.